ISSN 0036-0236, Russian Journal of Inorganic Chemistry, 2019, Vol. 64, No. 9, pp. 1146–1151. © Pleiades Publishing, Ltd., 2019.
Russian Text © The Author(s), 2019, published in Zhurnal Neorganicheskoi Khimii, 2019, Vol. 64, No. 9, pp. 965–970.

COORDINATION COMPOUNDS

Structure and Thermal Decomposition of Nd(III), Gd(III) and Tb(III) 2-Thiobarbiturates

N. N. Golovnev[a, *], M. S. Molokeev[a, b, c], and I. V. Sterkhova[d]
[a] *Siberian Federal University, Krasnoyarsk, 660041 Russia*
[b] *Kirensky Institute of Physics, Siberian Branch, Russian Academy of Sciences, Krasnoyarsk, 660036 Russia*
[c] *Far Eastern State Transport University, Khabarovsk, 680021 Russia*
[d] *Favorsky Institute of Chemistry, Siberian Branch, Russian Academy of Sciences, Irkutsk, 664033 Russia*
**e-mail: ngolovnev@sfu-kras.ru*

Received December 28, 2018; revised February 15, 2019; accepted March 15, 2019

Abstract—Complexes $[Ln_2(H_2O)_6(\mu_2\text{-Htba–O,O'})_4(\text{Htba–O})_2]_n$ (Ln = Tb (**I**), Gd (**II**), Nd (**III**); and H_2tba is thiobarbituric acid) have been synthesized. According to single-crystal X-ray diffraction, monoclinic crystals of **I–III** are isostructural. They contain three independent $Htba^-$ ions (one terminal and two bridging) and two independent Ln^{3+} ions. Six $Htba^-$ ligands (two terminal and four O,O'-bridging) and two water molecules are coordinated to one Ln^{3+} ion, and four O,O'-bridging $Htba^-$ ions and four water molecules are coordinated to the other Ln^{3+} ion to form square antiprisms. The antiprisms are bound by $Htba^-$ bridging ions into layers. Numerous hydrogen bonds and π–π interactions stabilize the structures of the compounds. Thermal decomposition of complexes **I** and **II** performed in air results in mixtures of oxides and oxysulfates, whereas complex **III** forms $Nd_2O_2SO_4$.

Keywords: lanthanide(III) 2-thiobarbiturates, structure, thermal stability

DOI: 10.1134/S0036023619090134

INTRODUCTION

The organometallic coordination polymers of lanthanides(III) possess high monochromaticity of luminescent radiation and are used in clinical diagnostics and biotechnology, organic light-emitting diodes, displays, optical amplifiers, and lasers [1–4]. One of the multifunctional ligands capable of forming coordination polymers of various structures with metal ions is 2-thiobarbituric acid (Fig. 1) [5]; its derivatives—thiobarbiturates—are used as drugs [6]. In the present work, continuing our systematic study of the structure and properties of 2-thiobarbituric and 1,3-diethyl-2-thiobarbituric lanthanide complexes [7–10], three isostructural complexes $[Ln_2(H_2O)_6(H_2tba)_6]$ (Ln = Tb (**I**), Gd (**II**), Nd (**III**)) have been prepared which possess potentially useful luminescent and magnetic properties [3, 4]. Their thermal decomposition in air has been studied.

EXPERIMENTAL

In this work, $TbCl_3 \cdot 6H_2O$, $GdCl_3 \cdot 6H_2O$, $Nd(NO_3)_3 \cdot 6H_2O$, H_2tba, and NaOH (chemically pure grade, Russian State Standard) were used without additional purification.

Synthesis of $[Ln_2(H_2O)_6(Htba)_6]_n$ (Ln = Tb (I), Gd (II), and Nd (III)). The hydrates of the lanthanide salts (0.463 mmol) were dissolved in water (10 mL) followed by the addition of solid H_2tba (0.200 g, 1.39 mmol). The mixture was neutralized with 1 M NaOH solution to pH 4. Fine crystalline precipitates **I** (yellow), **II** (red), and **III** (purple) were formed which were filtered off after 8 h. The yield of the compounds was 60–70%.

For $C_{24}H_{30}N_{12}Tb_2O_{18}S_6$ anal. calcd. (%): C, 22.4; H, 2.35; N, 13.1; S, 15.0.

Found for **I** (%): C, 22.1; H, 2.47; N, 12.8; S, 14.8.

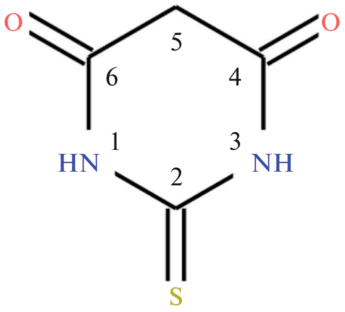

Fig. 1. Graphical formula of 2-thiobarbituric acid (H_2tba) molecule.

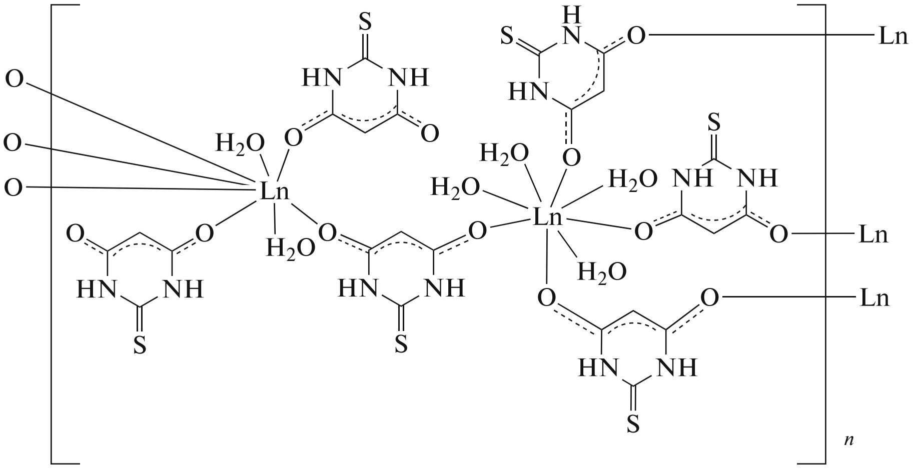

Fig. 2. Structure of complexes $[Ln_2(H_2O)_6(Htba{-}O,O')_4(Htba{-}O)_2]_n$.

For $C_{24}H_{30}N_{12}Gd_2O_{18}S_6$ anal. calcd. (%): C, 22.5; H, 2.36; N, 13.1; S, 15.0.

Found for **II** (%): C, 22.1; H, 2.55; N, 12.9; S, 14.7.

For $C_{24}H_{30}N_{12}Gd_2O_{18}S_6$ anal. calcd. (%): C, 23.0; H, 2.41; N, 13.4; S, 15.3.

Found for **III** (%): C, 22.7; H, 2.66; N, 13.0; S, 15.0.

In the course of slow evaporation of the mother solutions for 2–4 weeks, the corresponding single crystals were formed; the crystals were filtered off and dried in air between sheets of filter paper. The intensities of X-ray reflections from prismatic **I–III** crystals with sizes of 0.2 × 0.3 × 0.4 mm were measured at 100 K using a D8 VENTURE single crystal diffractometer (Bruker AXS, MoK_α radiation). The data were corrected for absorption using the SADABS program [11] by the multiscan method. The structure model was determined by direct methods and refined using the SHELXTL program package [12]. The positions of hydrogen atoms were determined from difference electron density syntheses, which were idealized and refined in the form associated with the main atoms. Table 1 shows the experimental parameters and the results of structure refinement.

The experimental powder X-ray diffraction patterns of fine-crystalline powders of **I–III** coincide with those theoretically calculated from X-ray diffraction data for the corresponding single crystals, which confirms their phase identity. A comparison of these powder X-ray diffraction patterns is shown in Fig. S1.

Structures of **I–III** were deposited with the Cambridge Structural Database (CCDC nos. 1576288, 1576438 and 1576287, respectively); the data are available free of charge at deposit@ccdc.cam.ac.uk or http://www.ccdc.cam.ac.uk/data_request/cif.

The thermal decomposition of the compounds was studied on an SDT-Q600 thermal analyzer combined with a Nicolet380 FT-IR spectrometer for the qualitative determination of gases emitted (air flow rate, 50 mL/min; heating rate, 10 K/min; temperature range, 24–850°C).

RESULTS AND DISCUSSION

Complexes **I–III**, together with $[Eu_2(H_2O)_6(Htba)_6]_n$ [7] and $[Sm_2(H_2O)_6(Htba)_6]_n$ [10], form a series of isostructural compounds $[Ln_2(H_2O)_6(Htba)_6]_n$. The independent part of their unit cells contains two Ln^{3+} ions in special positions, three $Htba^-$ ions, and three water molecules in general positions. The $Htba^-$ ions are coordinated to the Ln^{3+} cations only through O atoms. The two independent Ln^{3+} ions have different coordination environments (Fig. 2). The polyhedra $Ln(1)O_8$ and $Ln(2)O_8$ are square antiprisms connected to each other by bridging $Htba^-$ to form an infinite layer in the plane perpendicular to the direction $a + c$ (Fig. 3). As a result of the bridging O,O'-coordination of $Htba^-$ ions to Ln^{3+}, 24-membered cycles are formed. The structure of the complexes under consideration corresponds to the general formula $[Ln_2(H_2O)_6(Htba{-}O,O')_4(Htba{-}O)_2]_n$.

Main geometric characteristics of compounds **I–III** are given in the Appendix (Table S1). The Ln–O bond lengths fall in the range 2.3–2.5 Å and have usual values [13]. Like the unit cell volumes V (Table 1), the Ln–O bond lengths regularly increase when passing from compound **I** to **III**, which is explained by a monotonic increase in the crystallographic radius (r) of the Ln^{3+} ion [14]. The $[Sm_2(H_2O)_6(Htba)_6]_n$ [10] and $[Eu_2(H_2O)_6(Htba)_6]_n$ [7] structures were determined at different temperatures (296 and 300 K, respectively); therefore, the dependence of V on r for complexes $[Ln_2(H_2O)_6(Htba)_6]_n$ (Ln = Tb, Gd, Eu, Sm, Nd) was found to be nonmonotonic.

Table 1. Crystallographic data, details of data collection, and characteristics of data refinement

Parameter	**I**	**II**	**III**
Color	Yellow	Red	Violet
Molecular formula	$C_{24}H_{30}N_{12}O_{18}S_6Tb_2$	$C_{24}H_{30}Gd_2N_{12}O_{18}S_6$	$C_{24}H_{30}N_{12}Nd_2O_{18}S_6$
FW	1284.80	1281.46	1255.44
Space group, *Z*	$P2/n$, 2	$P2/n$, 2	$P2/n$, 2
a, Å	13.9922 (4)	14.026 (1)	14.1330 (8)
b, Å	10.0297 (3)	10.0613 (8)	10.1339 (6)
c, Å	15.3486 (5)	15.325 (1)	15.3565 (8)
β, deg	109.981 (1)	110.017 (2)	110.750 (2)
V, Å^3	2024.3 (1)	2032.0 (3)	2056.7 (2)
ρ_{calcd}, g/cm^3	2.108	2.094	2.027
μ, mm^{-1}	3.864	3.633	2.889
$2\theta_{max}$, deg	60.158	60.42	60.822
Number of reflections			
collected	59004	62552	62764
unique N_1 (R_{int})	5935 (0.0445)	5994 (0.0457)	6082 (0.0410)
with $F > 4\sigma(F)$, N_2	5566	5602	5562
h, *k*, *l* ranges	$-19 \le h \le 15$, $-14 \le k \le 14$, $-21 \le l \le 21$	$-19 \le h \le 19$, $-14 \le k \le 14$, $-19 \le l \le 21$	$-19 \le h \le 19$, $-14 \le k \le 14$, $-21 \le l \le 21$
Weight scheme for F^2	$w = 1/[\sigma^2(F_o^2) + (0.0202P)^2 + 4.4974P]$	$w = 1/[\sigma^2(F_o^2) + (0.0301P)^2 + 4.401P]$	$w = 1/[\sigma^2(F_o^2) + (0.0238P)^2 + 3.9105P]$
	$P = \max(F_o^2 + 2F_c^2)/3$		
Number of parameters to be refined	299	299	299
R (for N_1)	0.0223	0.0242	0.0255
R (for N_2)	0.0199	0.0213	0.0217
$wR(F^2)$ (for N_1)	0.0513	0.0581	0.0570
$wR(F^2)$ (for N_2)	0.0502	0.0565	0.0554
GOOF	1.055	1.012	1.121
Extinction coefficient	Not refined	Not refined	Not refined
$(\Delta/\sigma)_{max}$	<0.001	<0.001	<0.001
$\Delta\rho_{max}/\Delta\rho_{min}$, e/Å^3	0.529/−1.785	0.708/−2.043	0.707/−1.680

The geometric parameters of independent $Htba^-$ ions (one terminal and two bridging ones) in all three compounds coincide almost completely (Table S1), for example, the lengths of the C–O (1.257(2)–1.273(2) Å), C(4)–C(5), and C(5)–C(6) bonds (1.389(3)–1.398(3) Å) as well as C–S bonds (1.678(2)–1.684(2) Å) and the bond angle C(6A)C(5A)C(4A) (119.8°–119.9°).

In **I**–**III**, twelve hydrogen bonds N–H···O, N–H···S, O–H···O, and O–H···S are formed (Table S2), in which all $Htba^-$ ions and all water molecules are involved. Hydrogen bonds form a three-dimensional framework in which supramolecular motifs $R_2^2(8)$, S(6), $R_2^2(28)$, and $R_4^4(26)$ can be distinguished [15]. Using the PLATON program [16], the parameters of

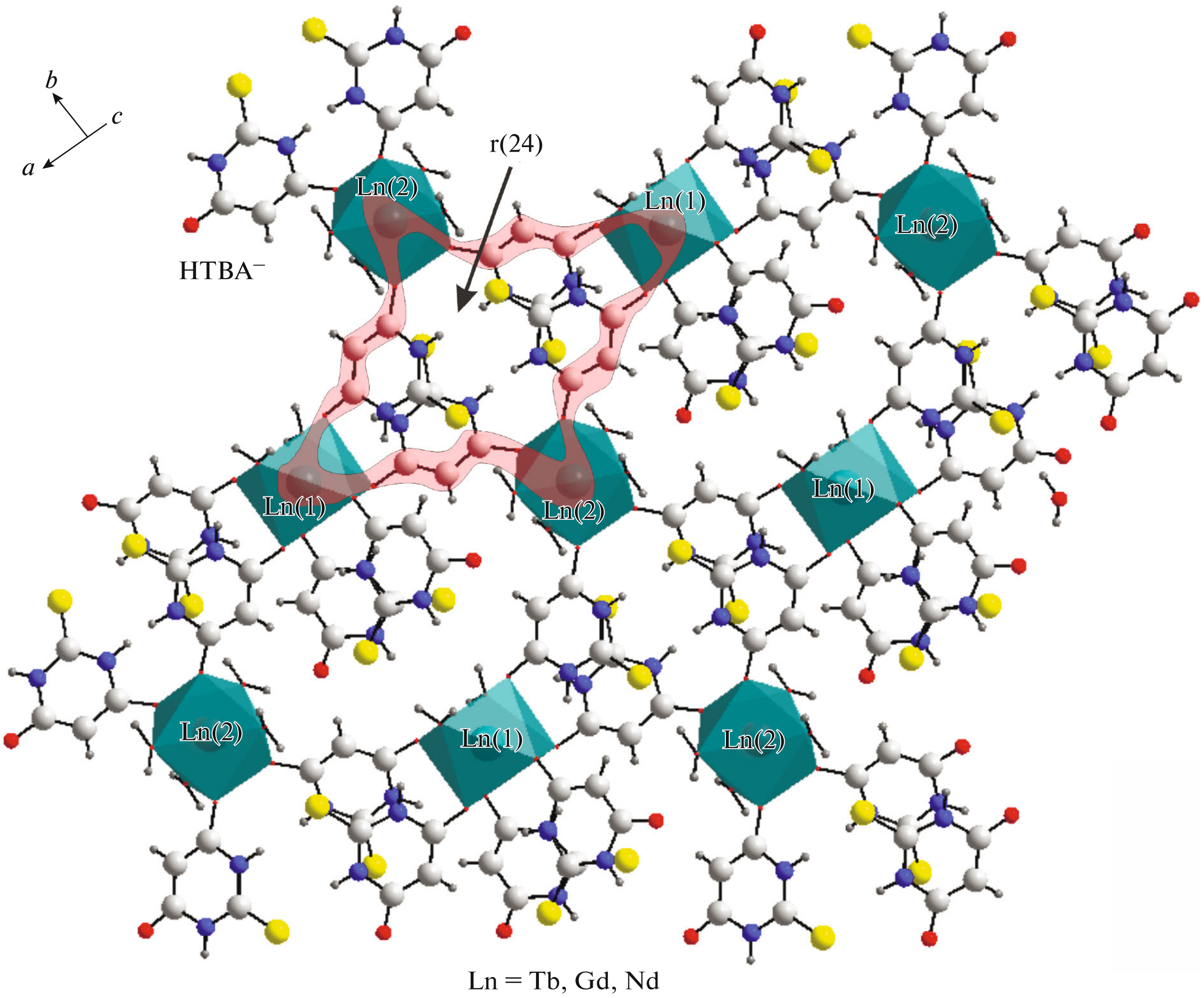

Fig. 3. Structure of the layer perpendicular to the direction *a* + *c*. The cyclic fragment of the structure is highlighted.

the π–π interaction between Htba⁻ ions (Table S3) were determined to belong to the head-to-tail type.

The thermal decomposition of compounds **I–III** proceeds in several stages (Fig. 4). At the first stage, the complexes are dehydrated to form crystalline phases that were not identified by powder X-ray diffraction. The experimental mass loss of substances (Δm_{exp}) was close to that calculated (Δm_{calcd}) assuming the removal of all six H_2O molecules (for **I** m_{exp} = 8.71%, m_{calcd} = 8.41%; for **II** m_{exp} = 9.03%, m_{calcd} = 8.50%; for **III**, m_{exp} = 8.60%, m_{calcd} = 8.61%). Dehydration is accompanied by endotherms on DSC curves (255°, 311° for **I**; 247° for **II**, and 246° for **III**). The oxidation of the organic ligand in **I–III** begins at ~300°C. In the range of 400–800°C, this process is accompanied by two or three exotherms and the evolution of H_2O, CO_2, COS, NO, and SO_2 gases. According to powder X-ray diffraction data, the final product of the decomposition of **III** at 800°C, as in the thermolysis of $[Nd(H_2O)_2(Htba)_2(CH_3COO)] \cdot 2H_2O$ [8], is pure $Nd_2O_2SO_4$ (Δm_{exp} = 33.0%, Δm_{calcd} = 33.2%). Oxysulfates $Ln_2O_2SO_4$ have a large capacity for oxygen atoms [17] and are promising as reaction catalysts for hydrogen production from CO and H_2O [18] resistant to sulfur poisoning. The thermal decomposition of **III** can be considered as an alternative method to prepare Nd(III) oxysulfate, which, in turn, can serve as a precursor for the preparation of Nd_2O_2S being a promising laser material [19]. The final products of decomposition of **I** and **II** are mixtures of the corresponding oxides and oxysulfates. The composition of the intermediate decomposition products of the compounds was not studied.

CONCLUSIONS

At 800°C, some thiobarbituric complexes are converted to $Ln_2O_2SO_4$ oxysulfates (Ln = Nd (complex **III**),

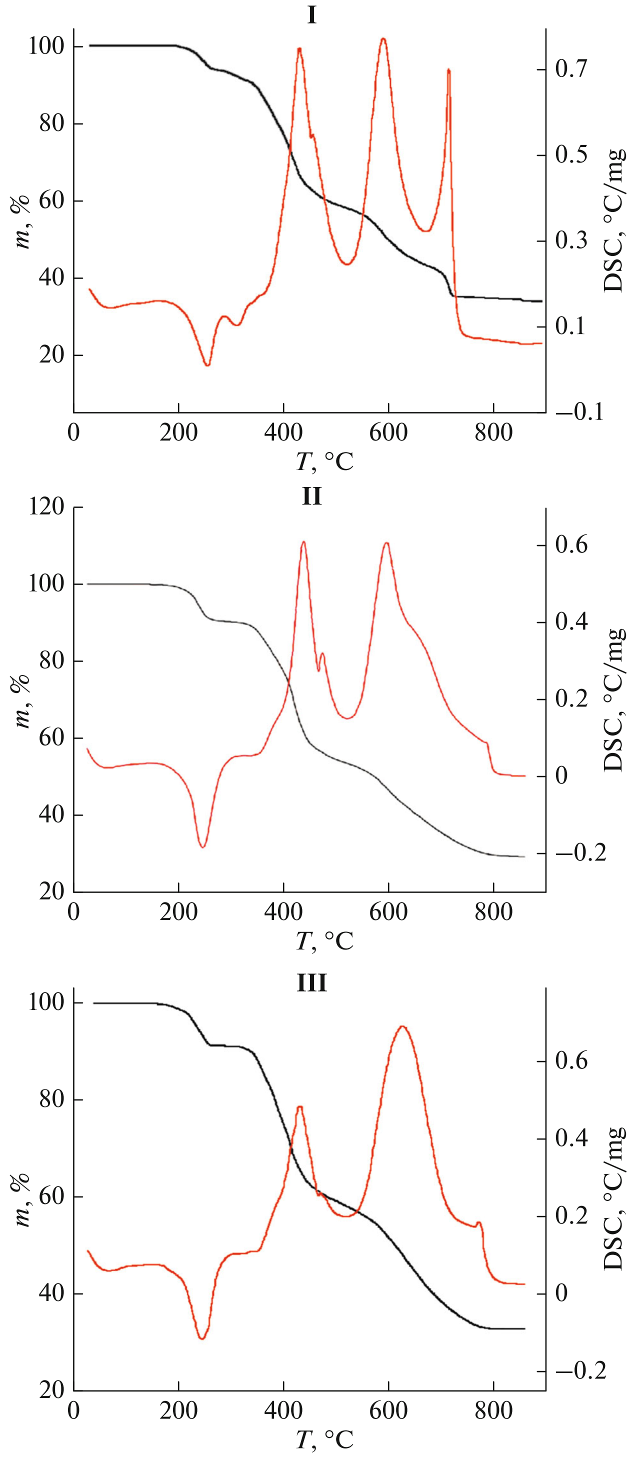

Fig. 4. TG and DSC curves for complexes **I**–**III** for their decomposition in air.

Sm [10], and Eu [7]), while others (**I** and **II**) transform to mixtures containing mainly oxides TbO_2, Tb_2O_3, and Gd_2O_3, respectively, and relatively small amounts of $Ln_2O_2SO_4$ (Ln = Gd, Tb). The different composition of the products of thermal decomposition of $[Ln_2(H_2O)_6(Htba)_6]_n$ can be explained by a decrease in the enthalpies of formation of Ln_2O_3 oxides with an increase in the lanthanide atomic number [20].

FUNDING

The work was performed as part of the State Assignment of the Ministry of Education and Science of the Russian Federation to the Siberian Federal University in 2017–2019. (4.7666.2017/BCh). The powder X-ray diffraction studies were performed using the equipment at the Baikal and Krasnoyarsk Centers for Collective Use of the Siberian Branch of the Russian Academy of Sciences.

SUPPLEMENTARY MATERIALS

Supplementary materials are available for this article at https://doi.org/10.1134/S0036023619090134 and are accessible for authorized users. Supporting information includes experimental, calculated, and difference powder X-ray diffraction patterns for **I**–**III** (Fig. S1); powder X-ray diffraction pattern for the product of decomposition of **III** (Fig. 2); bond lengths and bond angles for $[Ln_2(H_2O)_6(H_2tba)_6]_n$ (Table S1); geometric parameters of hydrogen bonds (Table S2); and parameters of π–π interactions of $Htba^-$ in the crystals.

REFERENCES

1. M. C. Heffern, L. M. Matosziuk, and T. J. Meade, Chem. Rev. **114**, 4496 (2014). https://doi.org/10.1021/cr400477t
2. Y. Yang, Q. Zhao, W. Feng, and F. Li, Chem. Rev. **113**, 192 (2013). https://doi.org/10.1021/cr2004103
3. S. Cotton, *Lanthanide and Actinide Chemistry* (Wiley, Uppingham, Rutland, 2006).
4. K. Binnemans, Chem. Rev. **109**, 4283 (2009). https://doi.org/10.1021/cr8003983
5. N. N. Golovnev and M. S. Molokeev, *2-Thiobarbituric Acid and Its Complexes with Metals: Synthesis, Structure, and Properties* (Sib. Feder. Univ, Krasnoyarsk, 2014) [in Russian].
6. M. D. Mashkovskii, *Medicines: A Manual for Doctors* (Novaya volna, Moscow, 2008) [in Russian].
7. N. N. Golovnev, and M. S. Molokeev, Russ. J. Coord. Chem. **40**, 648 (2014). https://doi.org/10.1134/S1070328414090036
8. N. N. Golovnev, M. S. Molokeev, S. N. Vereshchagin, and V. V. Atuchin, J. Coord. Chem. **68**, 1865 (2015). https://doi.org/10.1080/00958972.2015.1031119
9. N. N. Golovnev, M. S. Molokeev, and S. N. Vereshchagin, J. Struct. Chem. **57**, 167 (2016). https://doi.org/10.1134/S0022476616010200
10. N. N. Golovnev, M. S. Molokeev, I. V. Sterkhova, et al., J. Struct. Chem. **58**, 539 (2017). https://doi.org/10.1134/S0022476617030155
11. G. M. Sheldrick, SADABS, Version 2.01 (Bruker, Madison (WI), 2004).

12. G. M. Sheldrick, SHELXTL, Version 6.10 (Bruker, Madison (WI), 2004).
13. Cambridge Structural Database, Version 5.37 (Univ. of Cambridge, Univ. of Cambridge, Cambridge (UK), 2015).
14. R. D. Shannon and C. T. Prewitt, Acta Crystallogr., Sect. B **25**, 925 (1969). https://doi.org/10.1107/S0567740869003220
15. J. W. Steed and J. L. Atwood, *Supramolecular Chemistry*, 1st ed. (CRC, 2004; Akademkniga, Moscow, 2007).
16. *PLATON—A Multipurpose Crystallographic Tool* (Utrecht Univ., Utrecht, The Netherlands, 2008).
17. M. Machida, K. Kawamura, K. Ito, and K. Ikeue, Chem. Mater. **17**, 1487 (2005). https://doi.org/10.1021/cm0479640
18. I. Valsamakis and M. Flytzani-Stephanopoulos, Appl. Catal. **106**, 255 (2011). https://doi.org/10.1016/j.apcatb.2011.05.037
19. J. D. Lessard, I. Valsamakis, and M. Flytzani-Stephanopoulos, Chem. Commun. **48**, 4857 (2012). https://doi.org/10.1039/C2CC31105D
20. P. O. Andreev, E. I. Sal'nikova, and A. A. Kislitsyn, Russ. J. Phys. Chem. A **87**, 1482 (2013). https://doi.org/10.1134/S0036024413080050
21. F. A. Khamidov, I. U. Mirsaidov, and A. Badalov, Dokl. Akad. Nauk Resp. Tadzh. **57**, 676 (2014).

Translated by V. Avdeeva